Hybrid Luttinger liquid/Fermi liquid behaviour in an atomic wire on a surface

L. K. Dash* and A. J. Fisher†
Department of Physics and Astronomy, University College London, Gower Street, London WC1E 6BT
(Dated: February 1, 2008)

Recent advances in single atom manipulation have made it possible to create "wires" in the form of atomic scale linear structures on a semiconductor surface. If such structures are to be used in future electronic devices, it will be necessary to know to what extent they behave as one-dimensional conductors, in which the presence of electron-electron interactions in the wire lead to properties quite different from those found in higher-dimensional systems. In particular, it would be useful to know if these structures retain any of the Luttinger liquid properties that are predicted for a pure one-dimensional metal. However, experimental studies of such structures have so far yielded unclear and contradictory results. We investigate this problem theoretically by creating a highly simplified model of a wire on a surface—a chain of atoms that includes electron-electron interactions to represent the wire, coupled to a similar chain that excludes electron-electron interactions to represent, albeit crudely, the surface. We present results for the eigenstates and spectral functions for such systems that suggest that many Luttinger liquid indicators are present. However the system as a whole retains some residual Fermi liquid characteristics, and therefore merges properties of both one and higher dimensions.

PACS numbers: 71.10.Pm, 73.22.Lp, 74.20.Mn, 79.60.Jv, 81.07.Vb

I. INTRODUCTION

In recent years it has become possible to create atomic scale wires consisting of a single chain of atoms on a semiconductor surface. These wires have obvious potential applications in future nanoscale circuitry, but most of the research effort so far has concentrated on the electronic structure of these systems.

Moreover, it has been shown that certain of these systems are not subject to the Peierls transition, even at low temperatures. Hence they are expected to behave as one-dimensional metals, with properties substantially different from the Fermi-liquid properties of higher-dimensional metals. Specifically, the discontinuity of the occupation number at the Fermi energy is lost, spin and charge excitations become separated and the correlation functions of the system develop power-law behaviour. Experimental evidence for such Luttinger liquid-like behaviour has, however, proved elusive and ephemeral. In particular, the case of Au wires on vicinal Si(111) has attracted much recent discussion [1, 2, 3, 4, 5, 6], as have the potential Luttinger liquid properties of quasi-one-dimensional charge-transfer salts [7, 8, 9].

One of the important questions that remains unanswered is to what extent the coupling of the wire to the surface affects the one-dimensional properties that would be expected of an isolated wire. This is a somewhat more complicated problem than that of two coupled one-dimensional conductors, which has been widely studied [10, 11, 12, 13, 14, 15, 16, 17, 18, 19, 20, 21]

The present work therefore begins to tackle this problem by reducing it to its most simple form. The wire is represented as completely as possible, by a fully interacting one-dimensional conductor based on the Luttinger model. This is coupled to a one-dimensional representation of the surface, similar to the wire but without any electron-electron interactions. In this way we are able to probe the effects of the coupling of the wire to the surface in as simple a way as possible, while retaining many of the properties that would be found in a more realistic system.

In a previous paper [22] we described the case where the one-electron properties of the two chains are the same. In this paper we build on these results by treating the more relevant case in which the properties of the chain differ. Where relevant, we have reproduced results from this earlier work.

The remainder of this paper is structured as follows. We start with a review of Luttinger liquid theory, followed in section II B by a full description of our model and a justification of its choice. We then present results for the eigenstates of the system, both for two chains identical with respect to their non-interacting properties, and for two chains with differing properties. We then present results for calculations of the spectral functions for both types of systems, and calculate the Luttinger parameter K_ρ. The paper concludes with a discussion of the implications of the results.

II. THEORETICAL METHODS

A. The Luttinger model

Our calculations are based on Haldane's solution of the Tomonaga-Luttinger model [23], consisting of a chain of spinless idealized atoms with periodic boundary condi-

*Electronic address: louise.dash@ucl.ac.uk
†Electronic address: andrew.fisher@ucl.ac.uk

tions. The model is characterized by a linearized dispersion relation with slope $v_{\rm F}$ and a complete separation of the populations of left- and right-moving particles (as in figure 1) and the inclusion of an infinity of negative energy electrons [23, 24]. It is this that makes the model exactly solvable, as the boson commutation relations are then exact rather than approximate.

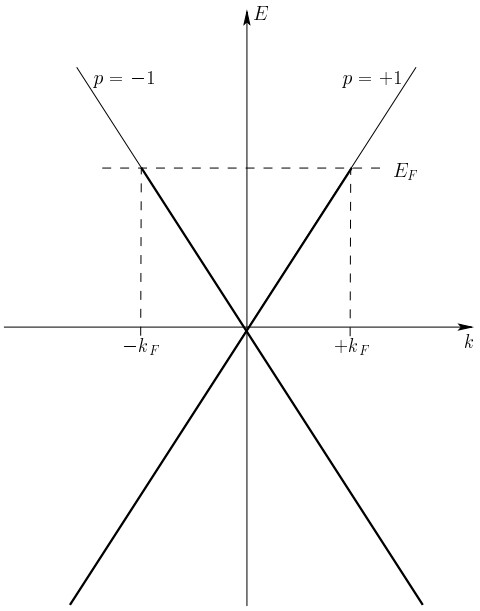

FIG. 1: Schematic representation of the Luttinger model. $p = +1, -1$ indicate the populations of left- and right-moving fermions respectively. States up to E_F are filled, this includes the infinity of negative energy states.

The details of the Luttinger model are covered in several review articles (see, for example, references [24, 25, 26]) and so we shall only review here those aspects of particular relevance to the current work. The total Luttinger model Hamiltonian can be split into three parts [24]:

$$\hat{H} = \hat{H}_0 + \hat{H}_2 + \hat{H}_4. \tag{1}$$

$\hat{H}_0$ represents the non-interacting part of the Hamiltonian:

$$\hat{H}_0 = \sum_{p,k} v_{\rm F}(pk - k_{\rm F}) : \hat{c}^\dagger_{pk}\hat{c}_{pk} :, \tag{2}$$

where q indicates momentum,p $(= \pm 1)$ the branch index and $: \ldots :$ implies normal ordering. The interaction parts of the Hamiltonian, $\hat{H}_2$ and $\hat{H}_4$, are given respectively by

$$\hat{H}_2 = \frac{2}{L}\sum_q g_2(q)\hat{\rho}_+(q)\hat{\rho}_-(-q), \tag{3}$$

$$\hat{H}_4 = \frac{1}{L}\sum_{p,q} g_4(q)\hat{\rho}_p(q)\hat{\rho}_p(-q). \tag{4}$$

The $\hat{H}_2$ term represents forward scattering between the left- and right-moving fermion branches, while the $\hat{H}_4$ term represents forward scattering within a momentum branch. The density operators $\hat{\rho}$ are defined in terms of the fermion operators as

$$\begin{aligned}\hat{\rho}_p(q) &= \sum_k : \hat{c}^\dagger_{p,k+q}\hat{c}_{p,k} : \\ &= \sum_k \left(\hat{c}^\dagger_{p,k+q}\hat{c}_{p,k} - \delta_{q,0}\langle\hat{c}^\dagger_{p,k}\hat{c}_{p,k}\rangle_0\right).\end{aligned} \tag{5}$$

The complete Hamiltonian can be diagonalized via a Bogoliubov transformation [23] to yield the bosonized form of the Hamiltonian

$$\tilde{H} = \frac{\pi}{L}\sum_{p,\ q\neq 0} v_0(q) : \tilde{\rho}_p(q)\tilde{\rho}_p(-q) : + \frac{\pi}{2L}\left[v_N\left(N_+ + N_-\right)^2 + v_J\left(N_+ - N_-\right)^2\right] \tag{6}$$

$$= \frac{1}{2}\sum_q \left(\omega_q - v_{\rm F}|q|\right) + \sum_q \omega_q \hat{b}^\dagger_q \hat{b}_q + \frac{\pi}{2L}\left(v_N N^2 + v_J J^2\right), \tag{7}$$

where the transformed density operators $\tilde{\rho}$ are related to the originals by a phase ϕ_q:

$$\tilde{\rho}_p(q) = \hat{\rho}_p(q)\cosh\phi_q + \hat{\rho}_{-p}(q)\sinh\phi_q. \tag{8}$$

There is a characteristic frequency $\omega_q = \sqrt{|(v_{\rm F} + g_4(q)/2\pi)^2 - (g_2(q)/2\pi)^2|/|q|}$ associated with the transformed bosons, while the quantum numbers $N \equiv N_+ + N_-$ and $J \equiv N_+ - N_-$ represent respectively the sum of the number of electrons on the positive and negative branches, and the difference between them (analogous to current).

The three velocities in the Hamiltonian are related as follows:

$$\begin{aligned} v_N v_J &= v_0^2, \\ v_N &= \frac{v_0}{K_\rho} = v_0 e^{-2\phi}, \\ v_J &= v_0 K_\rho = v_0 e^{+2\phi}, \end{aligned} \tag{9}$$

and are also related to the non-interacting Fermi velocity by

$$\begin{aligned} v_N &= v_\mathrm{F} + \frac{g_4 + g_2}{2\pi}, \\ v_J &= v_\mathrm{F} + \frac{g_4 - g_2}{2\pi}. \end{aligned} \tag{10}$$

The requirement that $\tilde{H}$ be a diagonalized version of $\hat{H}$ is ensured by the relationship between the Bogoliubov transformation phase ϕ_q and the interaction functions g_i:

$$e^{2\phi_q} = \left(\frac{\pi v_\mathrm{F} + g_4(q) - g_2(q)}{\pi v_\mathrm{F} + g_4(q) + g_2(q)} \right)^{1/2} \tag{11}$$

$$\equiv K_\rho(q). \tag{12}$$

The spinless Luttinger liquid parameter K_ρ is then obtained by taking the limit of $K_\rho(q)$ as q tends to zero. In all of the above the limit $q \to 0$ is implied where q is not explicitly included.

In addition there are two further parameters related to K_ρ: for a spinless Luttinger liquid they are given by

$$\alpha = \frac{1}{2}\left[K_\rho + \frac{1}{K_\rho} - 2 \right], \tag{13}$$

$$\gamma = 2\alpha. \tag{14}$$

The Fermi liquid corresponds to $K_\rho = 1$ and $\alpha = 0$ and so departures from these values can be used to "measure" the extent of non-Fermi liquid behaviour. α is an exponent which governs the power-law dependence of all single-particle properties (for example the density of states, which varies as $N(E) \approx |E - E_\mathrm{F}|^\alpha$), as well as other properties of the system, including the d.c. resistivity, which varies as $\rho(T) \approx T^{1-\gamma}$ [24, 27].

B. The model

We are now able to couple two Luttinger chains (labelled by superscript A and B) together by allowing hopping between adjacent points on each chain with matrix element $t_\perp$:

$$\begin{aligned} \hat{H}^\mathrm{coupled} = \hat{H}^A + \hat{H}^B \\ + t_\perp \sum_{x,p} \left(\hat{\psi}_p^{A\dagger}(x)\hat{\psi}_p^B(x) + \hat{\psi}_p^{B\dagger}(x)\hat{\psi}_p^A(x) \right). \end{aligned} \tag{15}$$

Other schemes of inter-chain hopping are of course possible, and we expect that they will generate similar results. We neglect any "drag effects" of inter-chain interactions that would be generated by interaction terms analogous to $\hat{H}_2$ or $\hat{H}_4$ involving electrons on both chains. We have the choice of using either a set of basis states generated by the diagonalized boson operators $\hat{b}_q^\dagger$ or the non-diagonalized operators $\hat{a}_q^\dagger$. We choose the latter, as although this has the consequence that the ground states for a single interacting chain no longer consist of the relevant zero-boson basis states, it is considerably more convenient computationally. The $\hat{\psi}^\dagger$ are fermion creation operators given in the bosonized form by

$$\hat{\psi}_{p,c}^\dagger(x) = \frac{1}{\sqrt{L}} e^{ipk_\mathrm{F}x} \left[e^{i\hat{\phi}_{p,c}^\dagger(x)} \hat{U}_{p,c} e^{i\hat{\phi}_{p,c}(x)} \right], \tag{16}$$

$\hat{\phi}_{p,c}(x)$ is a boson field operator given by

$$\hat{\phi}_{p,c}(x) = \left(\frac{p\pi x}{L} \right) N_{p,c} + i \sum_{q \neq 0} \theta(pq) \left(\frac{2\pi}{L|q|} \right)^{1/2} e^{iqx} \hat{a}_{q,c}, \tag{17}$$

where the subscripts p refers to the branch index (± 1) and c to the chain index. $\hat{U}_{p,c}$ is a ladder operator whose form ensures the anticommutation properties of the final fermion operator $\hat{\psi}_p^\dagger(x)$ despite the commutation properties of the constituent boson operators $\hat{a}_q$.

In order for $\hat{U}_{p,c}$ to produce anticommuting field operators on different chains, it is necessary to introduce a further phase factor into its definition, analogous to Haldane's phase factor $\zeta(p, N_p, N_{-p})$ for ensuring anticommutation between the branches of a single chain. The total ladder operator component of equation (16) thus takes the form

$$\hat{U}_{p,c} = \zeta(p, N_p, N_{-p})\zeta'(c, N_c, N_{-c}) | N_{p,c} + 1, N_{-p,c} \rangle, \tag{18}$$

where the subscript $c = \pm 1$ is a chain index. The anticommutation properties originate in the phase factors ζ, which can be written as

$$\zeta_{i=p,c} = (-1)^{(\frac{1}{2} i N_{-i})}. \tag{19}$$

This model provides us with a substrate that is metallic, whereas in reality we want to calculate for an insulating substrate. This may be achieved within the limitations of the Luttinger model in two ways. The first of these, reported here, is to adjust the Fermi velocity of the "substrate" chain so that the electrons preferentially reside on the "wire" chain. Our method of achieving this is described in detail in section III A. The second approach, to be reported elsewhere, is to move all the single-electron states associated with the substrate chain up in energy. This therefore has the effect of simulating a gap between the valence and (largely inaccessible) conduction bands of the substrate chain, while the states belonging to the wire chain are located within this gap.

C. Computational details

The choice of a specific form for the interactions $g_2(q)$ and $g_4(q)$ is arbitrary, as the Luttinger model remains completely solvable for any interaction that fulfils certain conditions [23]. We choose a Gaussian form for the interaction and set $g_2(q) = g_4(q) = 2\pi V(q)$ with

$$V(q) = I \exp\left(-2q^2/r\right) \tag{20}$$

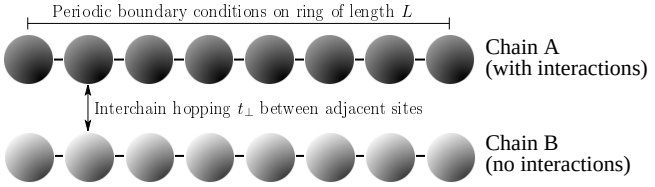

FIG. 2: Schematic representation of the two chain model. Electron-electron interactions are included on just one of the chains.

as this has the advantage that it maintains the same form in both real and momentum space. Other forms, such as a screened Coulomb interaction, would also be possible. The parameters I and r can be varied to control the "strength" and range of the interaction respectively. We complete the basic two chain model by setting the interaction strength on chain B, representing the substrate, to zero but retaining interactions on chain A.

The size of the computational Hilbert space is restricted by allowing only one boson in each mode. This does not affect the low energy properties in which we are interested, as we have checked that only higher energy excitations involve basis states with more than one boson in each mode. We also neglect the presence of the infinity of negative energy electrons, i.e. $\hat{c}|N_{\text{electrons}} = 0\rangle = 0$. However, we are still strongly limited in the size of the system we can handle: the Hilbert space scales exponentially with both length of chains and number of electrons. The largest system for which we have been able to calculate with arbitrary numbers of electrons is one with length $L = 6$ (i.e. 12 sites in total).

D. Spectral functions

We define the spectral function $\rho(q, \omega)$ as

$$\rho(q,\omega)_{p,c} = -\frac{1}{\pi}\Im\left[G^R_{p,c}(k_{\text{F}} + q, \omega + \mu)\right], \qquad (21)$$

with $q = k_{\text{F}} - k$, and the retarded Green's function $G^R_{p,c}$ defined as the double Fourier transform of

$$G^R_{p,c}(x,t) = -i\theta(t)\{\langle\hat{\psi}_{p,c}(x,t)\hat{\psi}^\dagger_{p,c}(0,0)\rangle\} \qquad (22)$$

where the subscripts p and c again indicate branch and chain indices. Whereas for a Fermi liquid we would expect $\rho(0, \omega)$ to be a delta function at the Fermi energy, the situation for a Luttinger liquid is quite different [28, 29, 30]. Spectral weight is repelled from the Fermi surface owing to the virtual particle-hole excitations generated by the inter-branch scattering term g_2, resulting in a broadened peak. As q is increased the Fermi liquid spectral function will merely broaden like q^2 reflecting the finite lifetime of electrons away from E_F, but for a Luttinger liquid there is zero spectral weight within a range $\pm v_0 q$ of the Fermi energy. In addition, the negative frequency contribution is suppressed exponentially with q, and for a continuum Luttinger liquid the positive frequency contributions have a power law dependence. For $\omega > 0$ this is of the form $\theta(\omega - v_0 q)(\omega - v_0 q)^{\gamma-1}$ and for $\omega < 0$ it is of the form $\theta(-\omega - v_0 q)(-\omega - v_0 q)^{\gamma}$, with γ given by equation (14) [24].

However, for our more complex system it is not easy to obtain an analytic form and so we resort to computational methods. We calculate the Green's function

$$\begin{aligned} G^R(k,k',\omega) = \langle N|\hat{c}_k\left[\omega - \hat{H} + \varepsilon_N\right]^{-1}\hat{c}^\dagger_{k'}|N\rangle \\ + \langle N|\hat{c}^\dagger_{k'}\left[\omega + \hat{H} - \varepsilon_N\right]^{-1}\hat{c}_k|N\rangle \end{aligned} \qquad (23)$$

using Haydock's tridiagonal Lanczos-based procedure [31, 32]. In order to ensure convergence, we put $\omega \to \omega + i\eta$, where η is an imaginary component of the energy roughly equal to the level spacing of the system [31]. $|N\rangle$ is the N-electron ground state, with energy ε_N. We also use the Lanczos method to calculate the eigenstates of the system.

III. RESULTS

A. Two types of system

Ideally, we would like to be able to calculate for a metallic chain coupled to an insulating chain representing the substrate. However, the metallic nature of our chains is inherent in the Luttinger model and so this is not possible with the present system. Nonetheless, we can reproduce some of the most important characteristics of such a system within the constraints of the current model. In particular, we are interested in systems where the Fermi velocities of the chains differ, i.e. the Fermi velocity for the interacting chain is less than that of the non-interacting chain, $v_F^A < v_F^B$. The result of this is that the electrons find it energetically preferable to reside on the interacting chain. This is one of the characteristics we would expect for a metal-semiconductor chain system, where the electrons in the wire are more mobile than those in the substrate. This has several consequences for the band structure of the coupled system, as can be seen more clearly in figure 3. The bands are not parallel and are not separated by $2t_\perp$, as they are for two chains with equal v_F The bands anticross at $E = 0$, which is E_F for our reference state of no participating electrons. Also, for similar chains, $v_F^A = v_F^B = v_F^{\text{bonding}} = v_F^{\text{antibonding}}$, whereas in this case we have $v_F^A (= 1.0) \approx v_F^{\text{bonding}} (= 1.002)$ and $v_F^B (= 2.0) \approx v_F^{\text{antibonding}} (= 1.998)$.

We now present our numerical results for these two systems—the first with $v_F^A = v_F^B$, the second with $v_F^A < v_F^B$. The quantities we calculate are those that may give us information about the Luttinger liquid properties of the system—specifically, the boson population of

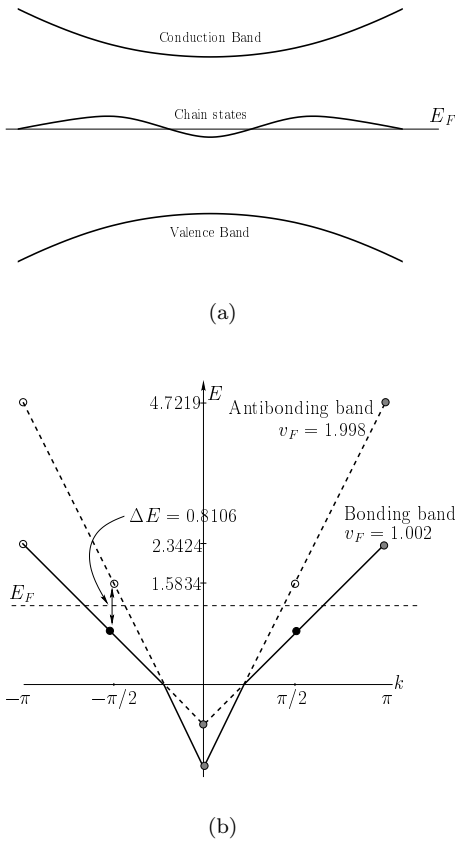

FIG. 3: (a) Schematic band structure of an atomic wire on a semiconducting surface, (b) Band structure as realised in our calculations for the non-interacting system with $L = 4$, $N = 2$, $t_\perp = 0.1$ $v_F^A = 1.0, v_F^B = 2.0$. Filled circles represent occupied states, unfilled circles empty states.

the eigenstates, the excitation energies and eigenstates, and the spectral function.

B. Boson contributions to eigenstates

Using the methods detailed above, we calculate the ground and neutral first excited states for our two systems at various interaction strengths. We first consider the boson population of these eigenstates. As we have chosen to work in the space of un-Bogoliubov transformed bosons, it is only the non-interacting ($I = 0$) systems that have a zero-boson population in all modes for the ground state. All the interacting systems ($I > 0$) have contributions from basis states that include bosons on one or both chains, as these basis states are not individually eigenstates of the interacting system. For both our two chain systems, contributions to the ground state may come from basis states with no bosons on either chain, bosons on the interacting chain (chain A) or bosons on both chains. These contributions are plotted in figure 4 as a proportion of the total ground state. Note that contributions from basis states with bosons on the non-interacting chain only are negligible and are not included.

For the case where both chains have equal Fermi velocities, as shown in figure 4(a), the data for basis states with bosons only on chain A maps almost exactly onto that for a single isolated chain. However, there is also a significant contribution from states with bosons on both chains which increases with I—the presence of interactions on chain A induces interaction effects on the otherwise non-interacting chain B. For stronger interchain coupling $t_\perp$, we see less of a contribution for both types, but nonetheless the data for bosonic states on chain A is still comparable to that of a single chain, indicating that for both $t_\perp = 0.1$ and $t_\perp = 0.5$ we are in a weakly coupled regime.

Figure 4(b) compares the results for the equal v_F system with those from the system with $v_F^A < v_F^B$. Once more, the data for bosonic basis states only on chain A matches the single chain data for both of our 2-chain systems. We again observe induced chain B boson states at a level similar to that for the equal v_F system in the $v_F^A < v_F^B$ system.

C. Charge distribution

We can also examine the distribution of charge between the two chains. Taking a simple case where there are just two electrons available for excitation, the possible distributions are both electrons on the interacting chain, one electron on each chain, or both electrons on the non-interacting chain. Those basis states where both electrons reside on the same chain may be thought of as "ionic"-like, and those where the electrons are shared between the chains as "covalent"-like. The charge distributions for the ground and first neutral excited states are shown in figures 5(a) and 5(b). We see that for the ground states of the equal v_F system, the eigenstates evolve smoothly from the non-interacting limit (where the charge distribution is has equal proportions of covalent and ionic states) to a situation at large values of I where the ground state is dominated by chain B ionic states. The presence of interactions on chain A has thus forced all the available charge onto the non-interacting chain B. The case of the excited states is, however, somewhat different. The $I = 0$ excited state is a fourfold degenerate combination of ionic and covalent states. Once even small chain A interactions are switched on, this degeneracy is lifted and the dominant basis states are covalent, as indicated by the discontinuity at $I = 0$ in figure 5(a). As I is increased, the role of the covalent basis states increases, but there is a further discontinuity in the charge distribution at $I \approx 2.0$, where the dominance of the covalent states is replaced by that of chain B ionic states. This is owing to a change in the nature of the excitation, from an inter-band excitation with $\Delta k = 0$ to an

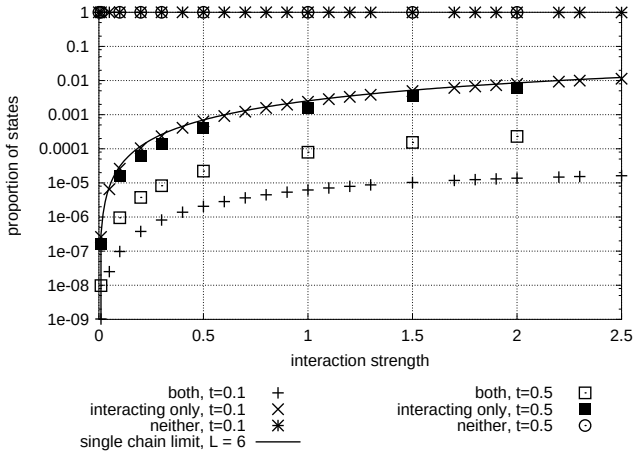

(a) $L = 6$, $v_F^A = v_F^B = 1.0$, $t_\perp = 0.1$ and 0.5. See also reference [22].

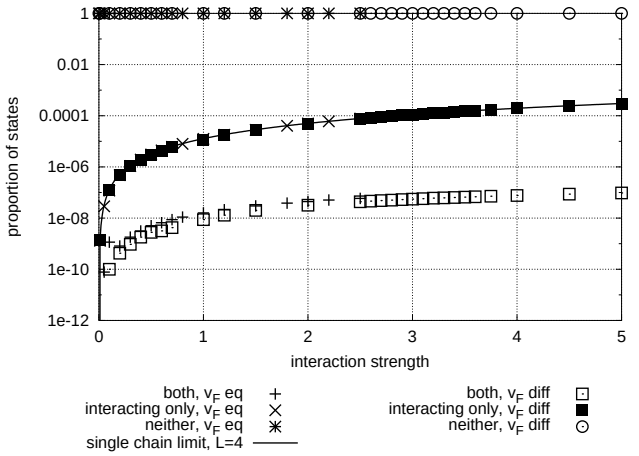

(b) $L = 4$, $v_F^A = 1.0, v_F^B = 2.0$ and $v_F^A = v_F^B = 1.0$ ($t_\perp = 0.1$)

FIG. 4: Contribution of bosonic basis states to the ground states as a function of interaction strength I.

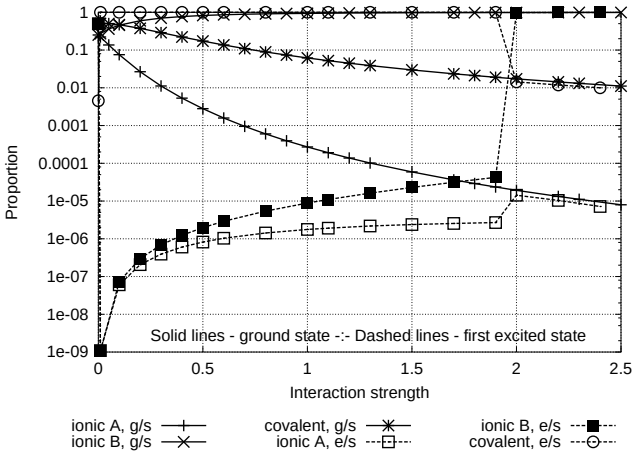

(a) $L = 6$, $v_F^A = v_F^B = 1.0$. See also reference [22].

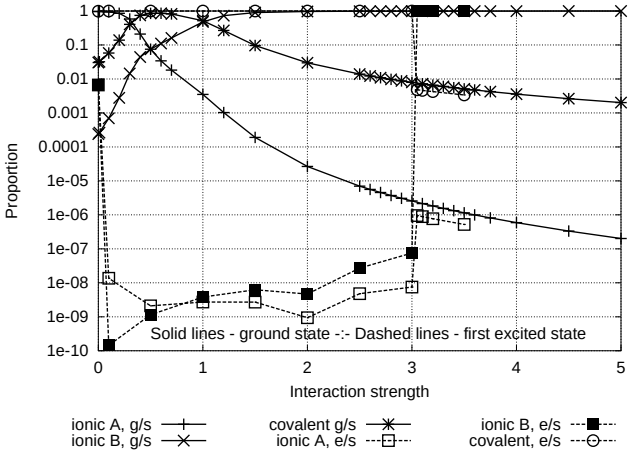

(b) $L = 4$, $v_F^A = 1.0, v_F^B = 2.0$

FIG. 5: Charge distribution within the chains for the ground state and neutral first excited state of the two-electron, two-chain model.

intra-band excitation with $\Delta k = 2\pi v_F/L$. For $I \geq 2.0$, the charge distribution for the excited state is very similar to that of the ground state, indicating that no net interchain hopping is involved in these excitations.

For the $v_F^A < v_F^B$ system, as shown in figure 5(b), the non-interacting ground state is dominated by chain A ionic state, with lesser contributions from covalent states and a minimal contribution from chain B ionic states. As I is increased, these evolve smoothly through a region ($0.5 \lesssim I \lesssim 1.0$) dominated by covalent states, to a situation, for $I \gtrsim 1.0$, where the system is dominated, like the equal v_F case, by chain B ionic states. The excited states exhibit a similar pattern of discontinuities to the equal v_F system, although the transition from inter-band to intra-band excitations now occurs at a higher interaction strength of $I = 3.0$.

Having examined the nature of the eigenstates, we now turn our attention to the eigenvalues, and in particular, to the neutral excitation energies. For the equal v_F system, the ground state energy, first neutral excited state energy and the excitation energy for various interaction strengths are calculated and shown in figure 6(a). In the non-interacting limit, the excitation energy ΔE is equal to $2t_\perp$, as would be expected for a transition between bonding and anti-bonding bands. As I is increased, ΔE also increases, until it becomes saturated at $I \approx 2.0$ at a value of $2\pi v_F/L$. This corresponds to the discontinuity in the charge distribution at $I \approx 2$ (figure 5(a)) already

associated with the change in nature of the excitation from inter- to intra-band.

For the system with $v_F^A < v_F^B$, however, the noninteracting ΔE is no longer $2t_\perp$ but is approximately 0.81, as indicated by the band diagram (figure 3). As I is increased, ΔE decreases and approaches zero in the range $0.5 \lesssim I \lesssim 1.0$, the same region as is dominated by the covalent states in the charge distribution. For $I \gtrsim 1.0$, ΔE once more increases until it too becomes saturated at $I \approx 3.0$, at a value of around 1.6. This is not, as might be suggested by the fact that all the charge is on the noninteracting chain, $2\pi v_F^B/L$, but is in fact slightly more than the value of $2\pi v_F^{\text{bonding}}/L$. The excitation energy also continues growing for $I > 3.0$, albeit very slowly: this, and the fact that ΔE is not exactly $2\pi v_F^{\text{bonding}}/L$ at saturation, is because of the combined effects of increase in energy due to induced boson states on chain B and increase in energy due to chain A interactions overtaking the effect of charge removal from chain A to chain B.

D. Spectral functions

The spectral functions for the model are now considered. Results for the calculation of the spectral function for both the equal v_F and the $v_F^A < v_F^B$ systems are presented in figure 7. For the equal v_F system, figure 7(a), there are three sources of broadening of the peaks away from the delta function we would expect for a Fermi liquid. The first of these is owing to the finite value of the imaginary energy η used in the numerical calculations, and leads to broadening of the peaks into Lorentzians with width $\sim \eta$. The second results from the splitting into bonding and antibonding bands due to the interchain coupling and is equal to $2t_\perp$. However, the remaining broadening, which is interaction-dependent, is due to the removal of spectral weight from the Fermi energy at $\omega = 0$, and is indicative of residual Luttinger liquid behaviour in the coupled system.

For the $v_F^A < v_F^B$ system, figure 7(b), we again see the broadening of individual peaks into Lorentzians. However, the peaks initially converge as I increases, analogous to the similar decrease in neutral excitation energy observed in the same region of $I \lesssim 0.5$. In this region around $I \sim 0.5$ however, two "branches" of the spectral function emerge, corresponding to separate peaks arising from covalent basis states and ionic chain B basis states—at lower values of I the covalent peak dominates, whereas for higher values of I the ionic B states become dominant. For the equal v_F spectral function, a similar analysis reveals that the single peak is due to ionic B states and there is no corresponding second peak arising from covalent states. The peak separation at $I = 0$ is approximately 0.81, consistent with that indicated by the band structure, and following the emergence of the two branches noted above, the peaks separate in the $I \gtrsim 1.0$ region, again indicating residual Luttinger liquid behaviour.

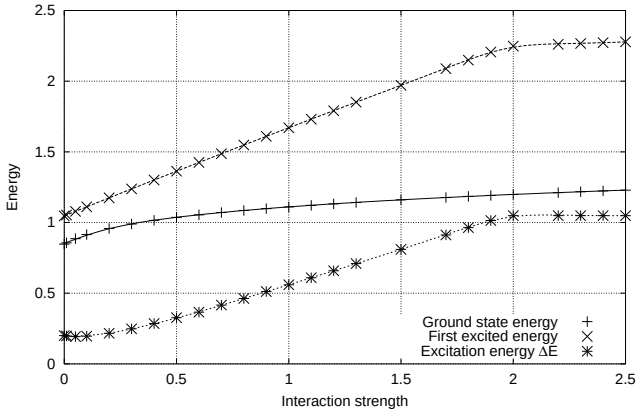

(a) $L = 6$, $v_F^A = v_F^B = 1.0$. See also reference [22].

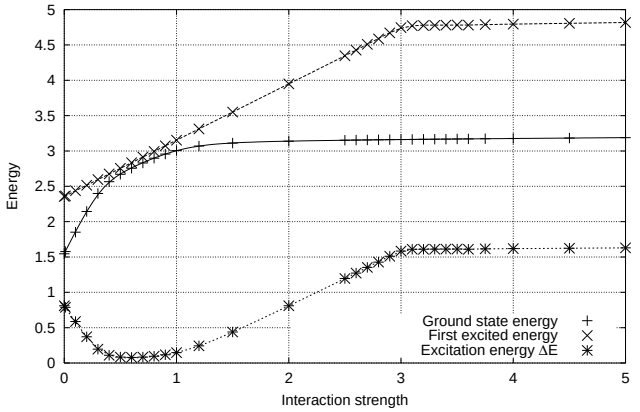

(b) $L = 4$, $v_F^A = 1.0, v_F^B = 2.0$

FIG. 6: Eigenvalues for the ground state and neutral first excited state of the two-electron, two-chain model.

E. Calculation of the Luttinger parameters

We can use the spectral function results to calculate the Luttinger parameters of the system. For a continuum system, this could be achieved by direct numerical measurement of the exponent α [28, 29, 30], but this is not possible in small discrete systems such as those under present consideration. However, we can define an effective Luttinger velocity v_0^{eff} for the system as follows. For a single Luttinger liquid chain, the separation $\Delta\omega$ of the electron and hole contributions to the spectral function is equal to $2v_0 q$, whereas for a non-interacting double chain system $\Delta\omega$ is equal to $2t_\perp$. We see from figure 7(a) that for the equal v_F system, we have a combination of both these effects, and hence define our effective v_0 in terms of the electron-hole peak separation

$$\Delta\omega = 2(v_0^{\text{eff}} + t_\perp). \tag{24}$$

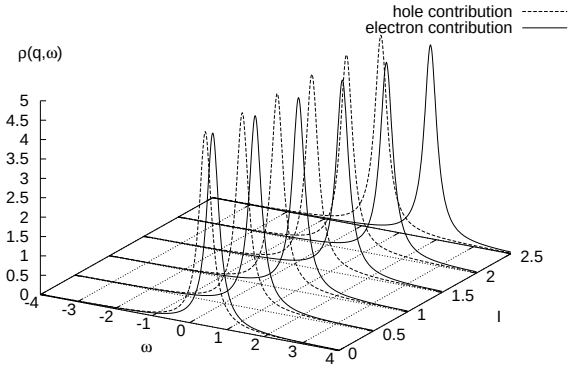

(a) $L = 6$, $v_F^A = v_F^B = 1.0$

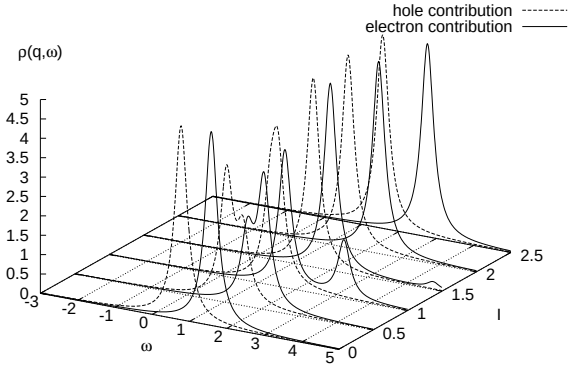

(b) $L = 4$, $v_F^A = 1.0, v_F^B = 2.0$

FIG. 7: Spectral functions $\rho(q = 0, \omega)$ for both types of two chain system. The hole and electron contributions have been renormalized to the same height in order to show the positions of the peaks accurately. Creation and annihilation both took place on chain A.

As we have chosen $g_2(q)$ to be equal to $g_4(q)$, we can equate equations (9) and (10) to give our effective Luttinger parameter

$$K_\rho^{\text{eff}} = e^{2\phi} = \frac{v_F}{v_0^{\text{eff}}}. \tag{25}$$

The results of this are shown in figure 10 and compared to the single-chain continuum limit.

However, for the $v_F^A \neq v_F^B$ system the situation is slightly different. In the non-interacting limit the bonding-antibonding splitting is no longer $2t_\perp$, but instead is of the order of $q|v_F^A - v_F^B|$. Since this is, in this case, much larger than $2t_\perp$, the bonding/antibonding splitting may be ignored, resulting in the following expression for the effective Luttinger velocity

$$v_0^{\text{eff}} = \begin{cases} \frac{\Delta\omega - 2t_\perp}{2q} & (v_F^A = v_F^B), \\ \frac{\Delta\omega}{2q} & |v_F^A - v_F^B| q \gg 2t_\perp. \end{cases} \tag{26}$$

We may then proceed as before to calculate v_0^{eff} and hence $K_\rho = v_F^{\text{SYSTEM}}/v_0^{\text{eff}}$ for this system.

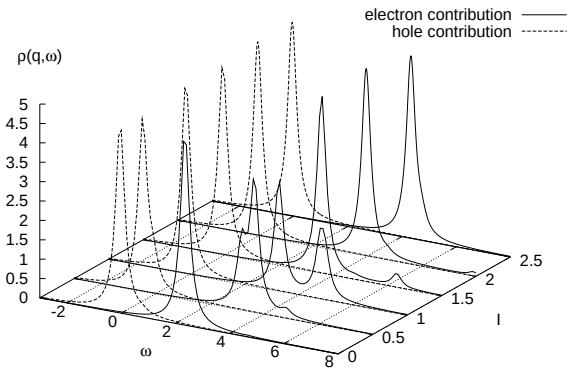

FIG. 8: Spectral function $\rho(q = \pi/L, \omega)$ for the $v_F^A = 1.0$, $v_F^B = 2.0$ two chain system. The hole and electron contributions have been renormalized to the same height in order to show the positions of the peaks accurately.

However, we note from figure 8 that there are two separate peaks in the electron part of $\rho(q, \omega)$. A decomposition of the basis states contributing to these states reveals that the lower energy peak is due to chain B-type ionic states, while the peak at higher ω is due to the covalent states, with virtually no contribution at all from the chain A ionic states. This is shown in figure 9. At lower interaction strengths, the covalent states dominate, but as the interaction strength increases, the chain B ionic state grow in importance and the ionic states decrease, fading completely by $I \approx 2.0$. The same phenomenon is responsible for the double peak structure in the hole contribution to $\rho(q = 0, \omega)$, where the effect is somewhat less pronounced.

Either of these peaks can be used to calculate K_ρ. Figure 10 shows the results for both the covalent and ionic peaks, together with the calculated Luttinger parameters for the $L = 4$ and $L = 6$ equal chain systems. The values for the continuum limit of a single chain are also shown for comparison. We can see that for $I \lesssim 0.5$, this system is more Luttinger liquid-like than the equal v_F system, but for interaction strengths greater than $I \gtrsim 1.0$, the covalent branch peters out and the system becomes less Luttinger liquid-like than the corresponding equal chain system.

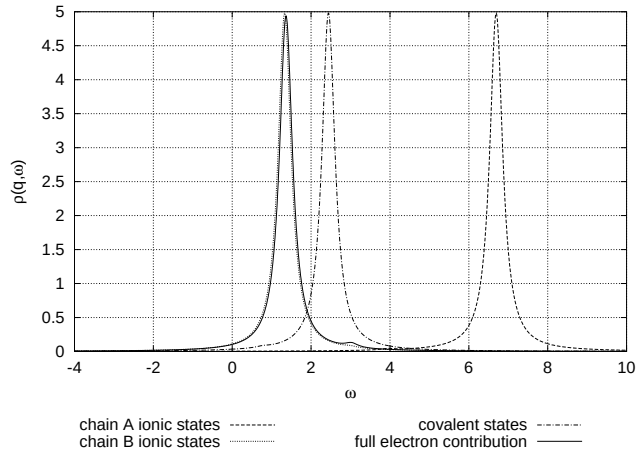

FIG. 9: Decomposition of the electron contribution to the spectral function into parts due to ionic chain A states, ionic chain B states, and covalent states. For the $L = 4$, $N = 2$, $t_\perp = 0.1$, $v_F^A = 1.0, v_F^B = 2.0$ system at $I = 0.7$.

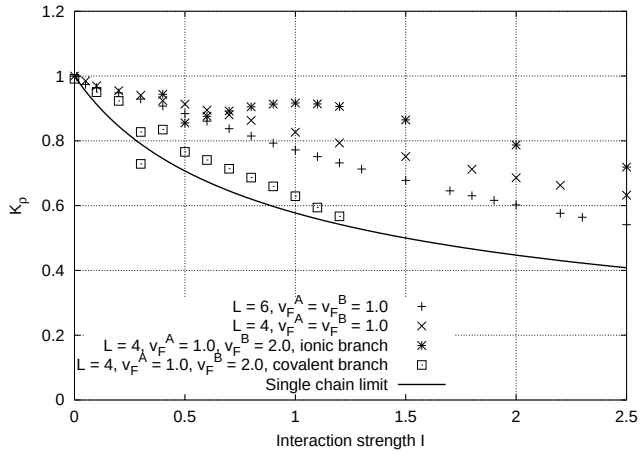

FIG. 10: Calculated values of the Luttinger parameter K_ρ for several systems. See also reference [22].

IV. CONCLUSIONS

The basic question we have asked in the current work is whether the coupling of an Luttinger liquid wire to a surface destroys any or all of its one-dimensional properties. We have attempted to answer this question purely by examination of the eigenstates and correlation functions of our, albeit simplified, model system. A more direct way of answering this question would be to measure the transport properties directly. However this would require substantial changes to the model which we believe would run the risk of obscuring the basic question: whether one-dimensional metallic systems coupled to surfaces *in general* retain their one-dimensional properties, regardless of the influence of such external sources as leads.

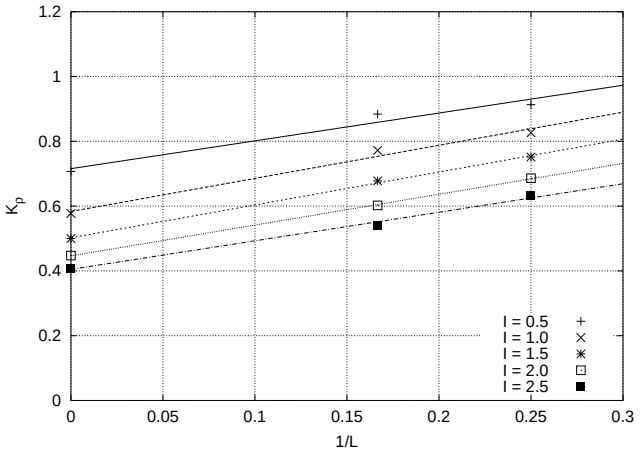

FIG. 11: Scaling with respect to inverse system length for the calculated values of K_ρ for the $v_F^A = v_F^B = 1.0$ system at various interaction strengths. The $1/L = 0$ data are for a single-chain continuum system.

We have presented results for a system of two chains, identical except for the presence of electron-electron interactions on one chain, representing the wire. We have shown that the coupling to the surface is weak in nature even for coupling parameters as high as $t_\perp = 0.5$, as the contribution to the ground state from basis states involving bosons remains comparable to that for an isolated Luttinger-liquid chain. We have seen that there is a fundamental change in the nature of the low-lying neutral excitations at a certain value of the interaction strength, owing mainly to the finite length of the chains. However, this shift, from inter-band excitations with $\Delta k = 0$ to intra-band excitations with $\Delta k = 2\pi v_F/L$ also leads to a transfer of charge away from the interacting "wire" chain to the non-interacting "substrate" chain, resulting in the restoration of some Fermi liquid properties. In particular the excitation energy in this region depends *not* on the Luttinger velocity v_0 but on the Fermi velocity v_F. However, the spectral properties, which depend on the nature of the charged rather than the neutral excitations, indicate that Luttinger liquid behaviour survives at values of the interaction strength not only below this threshold, but also above it. This behaviour manifests itself in the removal of spectral weight from the Fermi surface, and we have used this feature to calculate effective values of the Luttinger parameter K_ρ for our system.

Our calculated values of K_ρ indicate definitive Luttinger liquid behaviour for the system as a whole, and moreover, tend toward the values for an isolated continuum chain as the system length L increases. Figure 11 shows the scaling of K_ρ as a function of inverse system length for the equal-v_F system at various values of the interaction strength I. The values for K_ρ for an isolated continuum Luttinger liquid ($L = 0$) are included and a straight line fit is shown through all three data points. One would not expect a perfect straight line fit from these

data—the continuum single chain system remains, after all, substantially different in nature from a continuum two-chain system. However, the fact that the data are so linear with respect to inverse system length further reinforces our general conclusions.

In summary, therefore, we have investigated the problem of electron-electron interactions in an atomic scale wire on a surface. We have presented results that indicate that the resulting system does not behave as a pure Luttinger liquid but nonetheless retains many characteristics consistent with Luttinger liquid behaviour. It is clear from our results, however, that there is an important caveat to be borne in mind for hybrid systems such as this—that the results obtained depend very much on the properties of the system one chooses to measure.

Acknowledgments

The authors would like to thank Gillian Gehring for helpful discussions and suggestions. This work was supported financially by the UK Engineering and Physical Sciences Research Council and the National Physical Laboratory, Teddington, in the form of a CASE studentship. The calculations were performed on the Bentham Supercomputer at the HiPerSPACE Computing Centre, UCL, which is funded by the UK Engineering and Physical Sciences Research Council.

[1] P. Segovia, D. Purdie, M. Hengsberger, and Y. Baer, Nature **402**, 504 (1999).
[2] K. N. Altmann, J. N. Crain, A. Kirakosian, J.-L. Lin, D.Y. Petrovykh, F.J. Himpsel, and R. Losio, Physical Review B **64**, 035406 (2001).
[3] R. Losio, K.N. Altmann, A. Kirakosian, J.-L. Lin, D.Y. Petrovykh, and F.J. Himpsel, Physical Review Letters **86**, 4632 (2001).
[4] D. Sánchez-Portal, J. D. Gale, A. García, and R. M. Martin, Physical Review B **65**, 081401 (2002).
[5] F. Himpsel, K. Altmann, R. Bennewitz, J. Crain, A. Kirakosian, J.-L. Lin, and J. McChesney, Journal of Physics: Condensed Matter **13**, 11.097 (2001).
[6] I.K. Robinson, P.A. Bennett, and F.J. Himpsel, Physical Review Letters **88**, 096104 (2002).
[7] T. Lorenz, M. Hoffman, M. Grüniger, A. Freimuth, G. Uhrig, M. Dumm, and M. Dressel, Nature **418**, 614 (2002).
[8] A. Schwartz, M. Dressel, G. Grüner, V. Vescoli, L. Degiorgi, and T. Giamarchi, Physical Review B **58**, 1261 (1998).
[9] R. Claessen, M. Sing, U. Schwingenschlögl, P. Blaha, M. Dressel, and C.S. Jacobsen, Physical Review Letters **88**, Art. no 096402 (2002).
[10] S. Capponi, D. Poilblanc, and E. Arrigoni, Physical Review B **57**, 6360 (1998).
[11] D. G. Clarke and S. P. Strong, Journal of Physics: Condensed Matter **9**, 3853 (1997).
[12] D. G. Clarke and S. P. Strong, Physical Review Letters **78**, 563 (1997).
[13] N. Shannon, Y. Li, and N. d'Ambrumenil, Physical Review B **55**, 12963 (1997).
[14] S. Capponi, D. Poilblanc, and F. Mila, Physical Review B **54**, 17,547 (1996).
[15] D. Poilblanc, H. Endres, F. Mila, M. G. Zacher, S. Capponi, and W. Hanke, Physical Review B **54**, 10,261 (1996).
[16] D. Boies, C. Bourbonnais, and A.-M. S. Tremblay, Physical Review Letters **74**, 968 (1995).
[17] D. G. Clarke, S. P. Strong, and P. W. Anderson, Physical Review Letters **72**, 3218 (1994).
[18] M. Fabrizio, Physical Review B **48**, 15 838 (1993).
[19] M. Fabrizio and A. Parola, Physical Review Letters **70**, 226 (1993).
[20] A. M. Finkelstein and A. I. Larkin, Physical Review B **47**, 10 461 (1993).
[21] M. Fabrizio, A. Parola, and E. Tosatti, Physical Review B **46**, 3159 (1992).
[22] L.K. Dash and A.J. Fisher, Journal of Physics: Condensed Matter **13**, 5035 (2001).
[23] F. Haldane, Journal of Physics C **14**, 2585 (1981).
[24] J. Voit, Reports on Progress in Physics **58**, 977 (1995).
[25] J. Voit, *A brief introduction to Luttinger liquids*, cond-mat/0005114 (2000).
[26] J. Sólyom, Advances in Physics **28**, 201 (1979).
[27] M. Ogata and P. W. Anderson, Physical Review Letters **70**, 3087 (1993).
[28] K. Schönhammer and V. Meden, Physical Review B **47**, 16,205 (1993).
[29] J. Voit, Journal of Physics C **5**, 8305 (1993).
[30] V. Meden and K. Schönhammer, Physical Review B **46**, 15,753 (1992).
[31] R. Haydock, Solid State Physics **35**, 215 (1980).
[32] G. H. Golub and C. F. van Loan, *Matrix Computations* (Johns Hopkins University Press, Baltimore, 1996), 3rd ed.